REVIEW

Chemically converted graphene: scalable chemistries to enable processing and fabrication

Sanjeev Gambhir[1], Rouhollah Jalili[2], David L Officer[1,2] and Gordon G Wallace[1,2]

Graphene, a nanocarbon with exceptional physical and electronic properties, has the potential to be utilized in a myriad of applications and devices. However, this will only be achieved if scalable, processable forms of graphene are developed along with ways to fabricate these forms into material structures and devices. In this review, we provide a comprehensive overview of the chemistries suitable for the development of aqueous and organic solvent graphene dispersions and their use for the preparation of a variety of polymer composites, materials useful for the fabrication of graphene-containing structures and devices. Fabrication of the processable graphene dispersions or composites by printing (inkjet and extrusion) or spinning methods (wet) is reviewed. The preparation and fabrication of liquid crystalline graphene oxide dispersions whose unique rheologies allow the creation of graphene-containing structures by a wide range of industrially scalable fabrication techniques such as spinning (wet and dry), printing (ink-jet and extrusion) and coating (spray and electrospray) is also reviewed.
NPG Asia Materials (2015) 7, e186; doi:10.1038/am.2015.47; published online 5 June 2015

INTRODUCTION

Graphene that can be easily obtained from abundant natural or synthetic resources without significant energy consumption has the potential to breathe a new life into nanotechnology.[1] To realize this, the development of scalable chemistries is required that facilitate processing and fabrication in such a way that the inherent properties of graphene are maintained within material structures or devices. This will involve chemistries for the most part that enable efficient graphene integration with a host polymer, and that result in formulations with rheological properties that allow the use of fabrication tools such as fiber spinning or printing.[2–4] This report is a chemist's perspective on the methods developed for the production of graphene and graphene precursors, their integration into polymers and their fabrication into useful structures.

The impressive properties of this atom-thick sheet of aromatic carbons have created enormous interest in utilizing graphene in a wide variety of areas since Geim and Novoselov first demonstrated the mechanical exfoliation of graphene from graphite using Scotch tape, groundbreaking work that led to their award of the 2010 Nobel Prize in Physics.[5] Although this and other types of physical methods readily give sheets of graphene that can be used for fabricating various laboratory scale devices, it is chemical exfoliation methods that present the most likely opportunities for large-scale graphene production. As outlined in the resulting large number of reviews produced over the past 5 years, a wide variety of chemical methods for the production of graphene have been developed.[6] Reviews on graphene produced by chemical oxidation, the potential of such methods for production and its possible commercial applications have been prepared by Park et al.[6] and Kaner and co-workers.[7,8] Chemical exfoliation methods for the production of graphene have also been reviewed.[9,10] However, chemistries leading to scalable quantities of graphene in a form amenable to subsequent fabrication with or without integration into host polymer structures have not been adequately covered in reviews.

The properties of graphene needed for a specific application require a tailored approach to processing and fabrication. For example, chemical vapor deposition has predominantly been used to produce thin, highly conducting films for electronic/optoelectronics or bioelectronics[11] or for optically transparent films.[12–14] Chemically converted graphene (CCG) has been used to form electrodes for energy conversion (solar cells) and storage (batteries/capacitors),[15–23] industrial catalysis,[24] chemical and bio-sensing applications[25] as well as polymer composites with improved mechanical and electrical properties.[26,27] The difference in the kinds of applications suitable for each type of graphene preparation largely reflects the graphene sheet or platelet size produced, with mechanical or thermal exfoliation typically resulting in large single or several layer sheets that are challenging to handle and fabricate into devices, whereas chemical exfoliation produces smaller dispersible platelets that can be more readily processed and produced on a large scale. Chemical processing can also be used to produce large sheets of graphite oxide as stable dispersions. Such dispersions are amenable to fabrication and subsequent reduction to graphene.

[1]The Materials Node, The Australian National Fabrication Facility, Intelligent Polymer Research Institute, AIIM Facility, Innovation Campus, University of Wollongong, Wollongong, NSW, Australia and [2]ARC Centre of Excellence for Electromaterials Science, Intelligent Polymer Research Institute, AIIM Facility, Innovation Campus, University of Wollongong, Wollongong, NSW, Australia
Correspondence: Professor GG Wallace, ARC Centre of Excellence for Electromaterials Science, Intelligent Polymer Research Institute, AIIM Facility, Innovation Campus, University of Wollongong, Wollongong, NSW 2522, Australia.
E-mail: gwallace@uow.edu.au
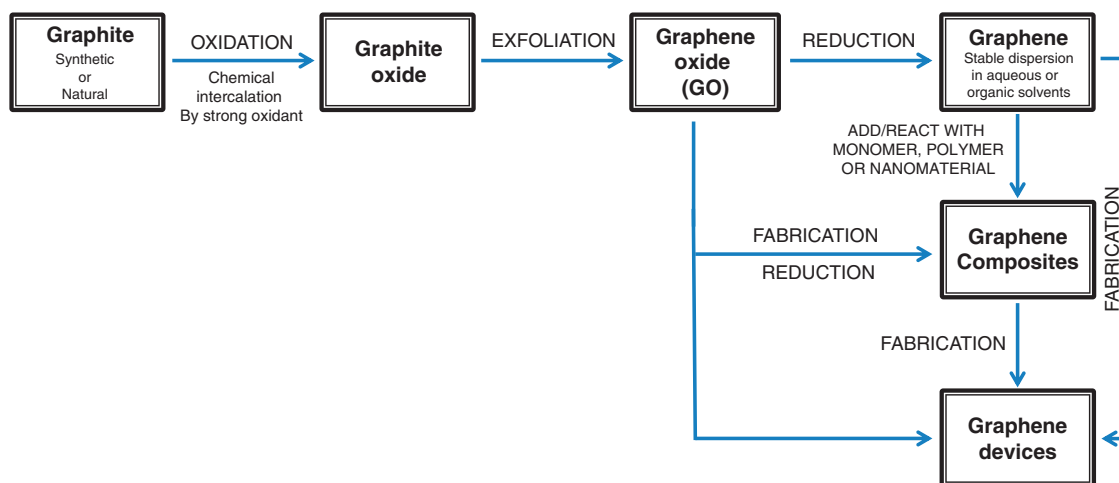Received 23 December 2014; accepted 2 March 2015

Figure 1 Steps involved in forming graphene composites or devices.

Within each of these approaches, there is a wide variety of preparation conditions. The key parameters that influence the steps involved in producing graphene from graphite and the processing as well as fabrication strategies that can be used to produce graphene containing composites or devices will be reviewed here.

The chemical production of dispersible graphenes is generally achieved through oxidation of natural or synthetic graphite to give graphite oxide that must be exfoliated to generate dispersible single sheets of graphene oxide (GO) (Figure 1). Reduction of this GO dispersion under carefully chosen conditions allows the reformation of the aromatic graphene sheets without aggregation to a graphitic-type multilayered structure. This dispersed chemically converted graphene or CCG can then be utilized to fabricate devices directly or via composite formation. While this approach generally produces an integrated graphenic material that is reasonably defect-free, a more common approach to composite and device formation has been to fabricate composites and devices with GO followed by a reduction step to produce the graphenic material (Figure 1). In this regard, the use of highly dispersed liquid crystalline GO (LCGO), a graphene precursor that can be readily processed and fabricated into a wide variety of structures using a number of different 3D fabrication methods, offers significant advantages.[4,28] The LCGO nanoplatelets are more than 10 times larger than the typical GO nanoplatelets affording highly ordered structures in solution and thus more viscous solutions for processing and fabrication. These larger nanoplatelets result from oxidation of natural graphite.

In the following sections, we discuss the differences in natural and synthetic graphite and the steps necessary to convert them into the graphene, and finally convert them into composites or other devices. We first explore the steps to enable processing and fabrication of the graphene form. Then we discuss the steps involved that enable processing and fabrication of GO, specifically LCGO, dispersions with subsequent reduction to graphene.

SOURCE MATERIAL: NATURAL VS SYNTHETIC GRAPHITE

Naturally occurring graphite is a mineral whose morphology can vary from micro-crystalline to macro-crystalline depending on its source and formation conditions.[29] It consists of graphitic carbon regardless of its crystalline perfection. The most common source of graphite used for chemical reactions, including its oxidation, is flake graphite, which is a naturally occurring mineral that is purified to remove heteroatomic contamination. The graphite content in the ore from which this material is obtained varies and range from 5 to 98% carbon depending on the source. The purity can be raised to 99.5% carbon, by means of mechanical separation and flotation. In order to achieve purities of >99.9% carbon that are a prerequisite for some applications like batteries, chemical (either acid or alkaline) or high-temperature treatment is required.

In contrast, synthetic graphites are all normally prepared by heating unstructured carbon at temperatures above 2500 °C. For example, Bay Carbon grade SP-1 graphite (Bay Carbon, Inc., Bay City, MI, USA) is obtained by the high temperature treatment of natural graphite. This heat treatment induces order into a graphitic structure and provides the high purity required for some specific applications. The characteristic of the synthetic graphite varies depending on the raw material and the heat treatment process used.[29]

The selection of graphite and subsequent processing depends on the final properties of the graphene required. Typically, processable and stable aqueous and organic dispersions of graphene platelets with sheet sizes $\leqslant 1\,\mu m$ are obtained by processing synthetic graphite or high purity micro-crystalline natural graphite using chemical oxidation and mechanical exfoliation route. In contrast, dispersions of larger sheets of GO and LCGO (20–50 µm) can be obtained from macro-crystalline natural graphite.

CHEMICAL INTERCALATION

In order to obtain single carbon layers, graphite must be intercalated to render it susceptible to exfoliation. Graphene layers in natural/synthetic graphite are stacked parallel on top of each other with a separation of 3.35 Å.[30] Although attraction between layers is not strong enough to prevent sliding in the direction of the *c* axis, they are sufficient to make it hard to exfoliate them as a single graphene sheet. Overcoming the van der Waals interactions is crucial for separation of the layers to produce single-layer graphene. Increasing the separation between adjacent graphene sheets by intercalation helps achieve this. The most successful strategy to exfoliate graphite is to weaken the van der Waals interactions by chemical intercalation followed by exfoliation.[31]

Intercalation of graphite can be achieved by exposing it to appropriate atoms or molecules that enter in between the graphene layers to form a graphite intercalation compound (GIC).[32] In this complex material, the intercalated compounds form a spacer layer. The number of graphene layers between two intercalated layers is called the stage, which is the most important and characteristic

Table 1 Comparison of different graphite sources, quantity of oxidant and its effect on the degree of oxidation and sheet size

Graphite source	Quantity of oxidant (moles)/ mole of graphite				Exfoliation method	Sheet lateral size (μm)	C/O (at. ratio)	Ref.
	H_2SO_4	$KMnO_4$	$NaNO_3$	$K_2S_2O_8$ $+P_2O_5$				
Dixon powdered flake (source unknown)	5.08	0.23	0.07	—	Not given	—	2.25	43
Bay Carbon SP-1 (Bay Carbon, MI, USA)	5.08	0.23	0.07	—	Ultrasonication	<1	2.7	111
Natural graphite GAK-2 (Zavalyevskiy Graphite, Kiev, Ukraine)	5.4	0.23	—	0.04	Ultrasonication	0.9–9	1.3	44
Graphite flake (Sigma-Aldrich, St Louis, MO, USA)	11	0.30	—	—	Stirring	>20	—	112
Graphite flake (Sigma-Aldrich, St Louis, MO, USA)	26.4	0.46	0.8 mole H_3PO_4		Stirring	—	—	49
Bay Carbon SP-1 (Bay Carbon, MI, USA)	5.4	0.23	—	0.04	Ultrasonication	<1	—	50
Natural graphite (Asbury Carbons, Asbury, NJ, USA)	24	0.76	—	—	Shaking	Mean = 32	1.3	56
Natural graphite (Asbury Carbons, Asbury, NJ, USA)	24	0.38	—	—	Shaking	Mean = 37	—	3
Graphite powder (Guangfu Fine Chemical, Tianjin, China)	5.2	0.45	0.14	—	Stirring	<1	—	113
Graphite flake (Sigma-Aldrich, St Louis, MO, USA)	29	0.30	—	—	Swirling	>100	—	114
Natural graphite, (Asbury Carbons, Asbury, NJ, USA)	3.86	1.7	—	—	Thermal expansion	<1	2.64	40
Graphite powder[a], ~ 100 mesh, 99.9995% (Alfa-Aesar, Heysham, Lancashire, UK)								47
1. GONS1	22	0.08	—	—	Ultrasonication (1 h)	0.5–0.6	3.68	
2. GONS2	22	0.15	—	—	Ultrasonication (1 h)	0.5–0.7	3.06	
3. GONS3	22	0.23	—	—	Ultrasonication (1 h)	≤0.2	2.31	
Graphite ⩾ 99.5%[b] (Source unknown)								48
1. HGTO[c]	5.9	0.23	0.07	—	Ultrasonication (0.5 h)	Mean = 1.456	2.33	
2. MGTO1[d]	5.9	0.23	0.07	—	Ultrasonication (0.5 h)	Mean = 1.447	2.28	
3. MGTO3[e]	5.9	0.23	0.07	—	Ultrasonication (0.5 h)	Mean = 1.520	2.25	

[a]Graphite oxidized using different quantities of oxidants.
[b]Oxidized under different conditions of reaction temperature.
[c]Addition of reactants was done at low temperature and then the reaction temperature was raised to 35 °C and maintained for 2 h.
[d]Addition of reactants was done at low temperature and then the reaction temperature was raised to 60 °C for 15 min.
[e]Addition of reactants was done at low temperature and then the reaction temperature was raised to 45 °C and maintained for 1 h.

ordering property of GIC. The first report on the synthesis of GIC was in the early 1840s but the first systematic investigations did not begin until after the introduction of X-ray diffraction methods in the early 1930s. However, it was only in the past few decades that the research on GICs has become a field of intense activity in both academia and industry. The synthesis and characterization of GICs has been the subject of several review articles, where a large number of intercalators (>100) are discussed.[32,33] Generally, the intercalants can be classified based on their interaction with graphite, whether they form donor compounds such as alkali metals or acceptor compounds such as sulphuric and nitric acids.

Intercalation of graphite with potassium, KC_8, has been achieved by reacting stoichiometric amounts of potassium with graphite overnight at 200 °C.[34] The product which is a bright gold powder was used to produce graphite nanoplatelets on the order of 2–150 nm thickness. The other most common intercalation method, is stirring natural graphite with a mixture of concentrated sulphuric acid and nitric acid (4:1, v/v) for 16 h at room temperature to obtain graphite bisulphate.[35,36] Reacting graphite with strong acid (H_2SO_4) and strong oxidant ($KMnO_4$), known as the modified Hummers method, is another common method used to obtain predominantly stage 1 GIC.[37] In the graphite bisulphate, the graphite structure remains mainly intact because the guest molecules are only located in between the carbon layers, whereas chemical intercalation with a strong oxidant negatively affects the graphite's electronic properties as its conjugated sp^2 structure is disrupted. Intercalation is also possible using milder conditions through co-intercalation with iron chloride ($FeCl_3$) and

nitromethane (CH_3NO_2).[38] In this method, iron chloride, a mild oxidant, facilitates the intercalation of nitromethane between the graphite layers without degrading the integrity of the graphene sheet in contrast to the stronger oxidative conditions in which strong acid and oxidant are employed for intercalation.[39,40]

OXIDATION OF GRAPHITE

Chemical intercalation of graphite using strong oxidant to produce graphite oxide is the most common method for graphite intercalation. There have been a wide variety of different approaches reported for the oxidation of graphite including chemical and electrochemical oxidation. Two approaches have been typically used to obtain processable CCG, the most common being the oxidation of graphite to give graphite oxide (Figure 1). Graphite oxide, after purification is exfoliated to give GO as a stable dispersion and is subjected to reduction to give a CCG dispersion. The use of strong chemical oxidants leads to a high degree of defects in the graphitic structure resulting in a highly oxidized GO. Subsequent selective reduction of GO results in the removal of the majority of basal plane defects with retention of the peripheral anionic functionalities that ensure dispersion of the CCG. Alternatively, careful selective oxidation of graphite using considerably milder oxidation conditions can result in the introduction of just enough anionic functionalities on the graphenic structure to allow dispersion of the CCG.[41]

The oxidation of graphite reported by Brodie in 1859 and modified by Staudenmaier et al.[42] in 1899 used $KClO_3$, nitric acid (>90%) sulphuric acid, and was time consuming and hazardous.

Table 2 Varying the extent of graphite oxidation and different exfoliation approaches resulting in GO

Graphite	C/O ratio	Exfoliation method/ medium	Time of exfoliation (min.)	Lateral size (µm)/height profile by AFM (nm)	Efficiency of exfoliation (%)	Ref.
Graphite powder, ~ 100 mesh, 99.9995%	3.68[a]	Ultrasonication/H_2O	60	0.5–0.6/2.1–2.5	40	47
(Alfa-Aesar, Heysham, Lancashire, UK)	3.06[a]		60	0.5–0.7/1.0–1.2	90	
	2.31[a]		60	⩽0.2/0.9–1.2	100	
Graphite (99.5%, ~ 30 µm)	2.33[b]	Ultrasonication/H_2O	30	1.5/0.9–2.3	90.0	48
(source unknown)	2.28[b]		30	~ 1.5/1.0	50.2	
	2.25[b]		30	~ 1.5/1.0	95.8	
Natural graphite, z-5F (Ito Graphite Industries, Japan)	—	Rapid freeze–thaw method/H_2O	Six freeze–thaw-centrifugation cycles	~ 3/1.0	80	54
Expandable graphite oxide from expandable graphite (Qing Dao Graphite Company, China)	2.7	Ultrasonication/DMF	60	~ 1–4/1.0	100	51
Bay Carbon SP-1 (Bay Carbon, MI, USA)	2.4	Ultrasonication/H_2O	0.0	10/1.0	—	53
			10.0	1/1.0	—	
			30.0	0.5/1.0	—	
			90.0	0.25/1.0	—	
			900.0	0.10/1.0	—	
Natural graphite	1.3	Self-exfoliation/H_2O	Centrifugation[c]	⩾37/0.83	Fully exfoliated	52
(Asbury Carbons, Asbury, NJ, USA)		Self-exfoliation/DMF	Centrifugation[c]	⩾12/1.1	Fully exfoliated	
		Self-exfoliation/CHP	Centrifugation[c]	⩾20/1.0	Fully exfoliated	
		Self-exfoliation/THF	Centrifugation[c]	⩾10/0.92	Fully exfoliated	
		Self-exfoliation/Acetone	Centrifugation[c]	⩾17/0.86	Fully exfoliated	
		Self-exfoliation/EtOH	Centrifugation[c]	⩾15/0.83	Fully exfoliated	

Abbreviations: AFM, atomic force microscopy; CHP, *N*-cyclohexyl-2-pyrrolidone; DMF, dimethylformamide; THF, tetrahydrofuran.
[a]Oxidation of graphite with increasing amounts of $KMnO_4$.
[b]Oxidation of graphite under varying conditions of temperature and time.
[c]Aqueous dispersion of graphene oxide is repeatedly centrifuged and washed with selected solvent (6 times for 10–30 min at 11000 r.p.m.) for self-exfoliation and stable dispersion.

Hummers *et al.*[43] developed a safer method that involved reacting natural graphite with a mixture of $NaNO_3$, $KMnO_4$ and concentrated H_2SO_4, to achieve the required high levels of oxidation. In order to obtain a fully oxidized GO, Kovtyukhova *et al.*[44] established a two-step oxidation of graphite, initially treating the graphite with concentrated H_2SO_4, $K_2S_2O_8$ and P_2O_5 followed by oxidation using Hummers method.[45,46] These three methods comprise the primary routes for forming GO. As summarized in Table 1, a myriad of approaches to graphite oxidation have emerged. The product obtained varies according to the nature of the oxidant, the graphite source and the reaction conditions employed. The oxidation step and associated clean up to remove excess reactants and products is time consuming requiring many hours to days to complete.

Tailoring the degree of oxidation is important since the GO obtained by using excessive oxidant quantities or harsh oxidation conditions has more defects leading to significant distortions of the graphene lattice Exfoliation of highly oxidized graphite oxide predominantly results in monolayer of GO and the efficiency of exfoliation is improved but the lateral size of the sheets is reduced (Table 1 and Table 2). Over-oxidized GO, though more dispersible in aqueous media, requires harsher reduction conditions to restore the graphene basal aromatic structure and thus conductivity.[47,48]

However, Tour *et al.*[49] have shown that replacing sodium nitrate by phosphoric acid and increasing the amount of $KMnO_4$ in a modified Hummers oxidation of graphite affords a more oxidized and hydrophilic GO with no toxic gas production or large exotherm. The resulting CCG obtained from the hydrazine reduction of the GO is comparable in quality and conductivity with that of CCG from a typical Hummers produced GO, making this an attractive approach for large-scale graphene production.

A reduction in the quantity of oxidants and alternate oxidation processes such as that developed by Tour[49] are the key to future bulk processing of CCG production.

EXFOLIATION OF GRAPHITE OXIDE

The exfoliation of graphite oxide to give stable dispersions of GO followed by reduction of the GO to graphene, provides a facile route to the large-scale processing of graphene-based materials.[9,50] The extent of oxidation and choice of exfoliation procedures used are critical for controlling the efficiency of exfoliation, lateral sheet size as well as the number of GO layers (Table 2).[47,48,51–55] As the oxygen content increases in the starting graphite oxide, the efficiency of exfoliation also increases.[47] For example, in their study of the capillary zone electrophoresis of GO, Mueller *et al.*[53] exfoliated graphite oxide using high dilution at different intervals of ultrasonication over 15 h. As observed in the atomic force microscopy images of the resulting GO, the lateral size reduced over that time from the initial 10 µm to 100 nm.

The exfoliation of graphite oxide in aqueous medium is very much dependant on the pH and ionic strength of the medium. Usually neutral to basic pH and low ionic strength is preferred and this has been achieved by repeated washing/dialysis of graphite oxide.[16,56–58]

The primary method of exfoliation of GO is ultrasonication in aqueous,[50] binary[59] or organic solvents;[51] however, spontaneous exfoliation of extra-large sheets of GO to form stable dispersions in different solvents has also been achieved.[2,3,52,56,58,60]

Ogino *et al.*[54] reported the exfoliation of graphite oxide in water without sonication. The authors used a new approach of rapid freezing of an aqueous solution containing graphite oxide and subsequent thawing of the resultant solid. The GO synthesized under these milder exfoliation conditions has a lateral size at least threefold higher than
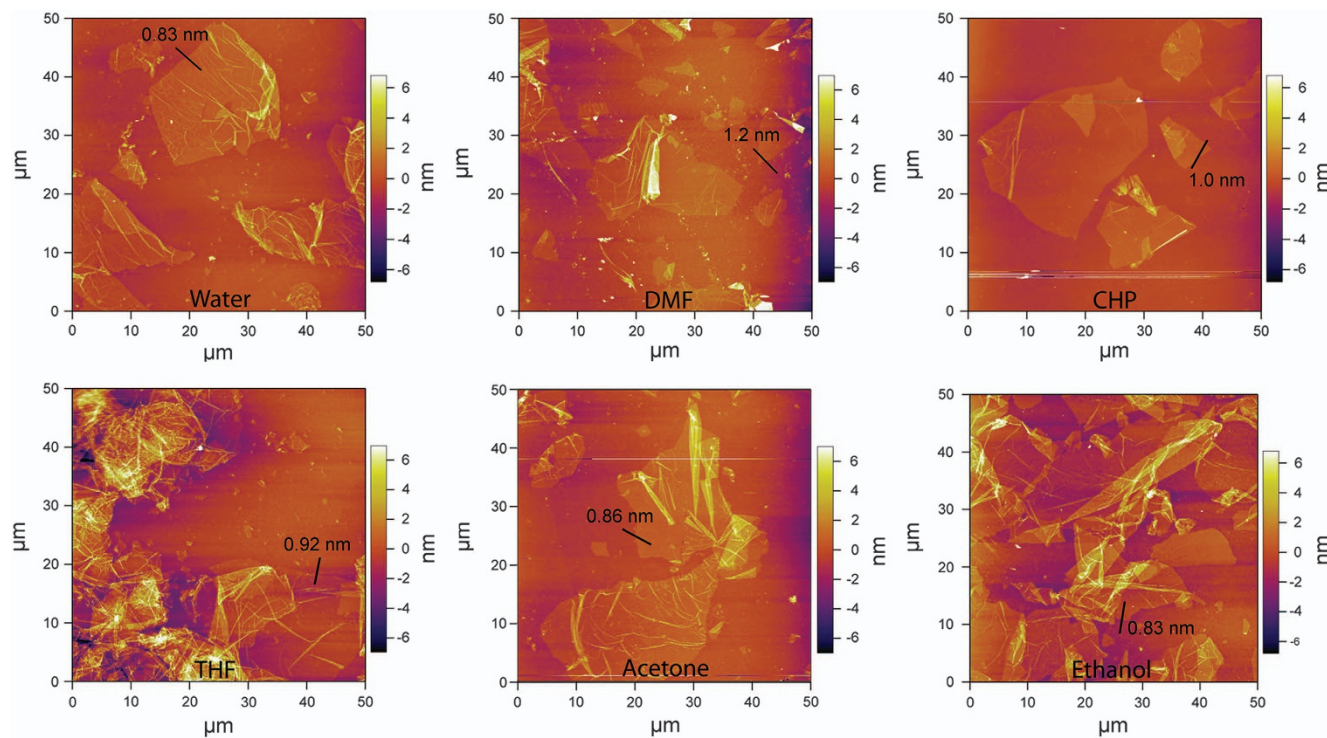
Figure 2 Atomic force microscopy images of graphene oxide sheets prepared from various organic solvent. The marked line in each image shows the measured thickness of the sheet. Reprinted with permission from Jalili *et al.*[52] Copyright 2013 American Chemical Society.

that of GO prepared using sonication (Table 2). Stankovich *et al.*[61] considered the strong hydrophilicity of GO was the barrier for the formation of GO nanoplatelets in organic solvents, and discovered that isocyanate functionalization led to GO dispersion in organic solvent.

Jalili *et al.*[52] have demonstrated exfoliation of ultra-large GO sheets in both water and a wide range of organic solvents, overcoming the practical limitations imposed on obtaining individual GO sheets with larger sheet sizes for nonaqueous applications. This involved the use of several washing steps followed by centrifugation to change the phase from aqueous to other polar solvents, confirming the exfoliation of the monolayer GO in each medium (Figure 2) by atomic force microscopy imaging. Step height measurements performed on the samples indicated that all of the samples contained single-layer GO sheets; as the mean measured height was between 0.8 and 1.2 nm depending on the solvent used. The thickness of a monolayer of graphene is ~ 0.34 nm, however, GO has functional groups that act as pillars giving rise to the larger measured height. Hydrogen bonding of each solvent molecule with GO results in different apparent sheet thicknesses depending on the solvent molecular size and arrangement on the surface of GO sheets.

REDUCTION OF GRAPHENE OXIDE

Procedures used for the reduction of GO have been extensively reviewed.[9,10,55] Reduction strategies include thermal, chemical and multistep reduction procedures. Thermal reduction has been initiated by convective heating, microwave or photo-reduction and for chemical reduction, numerous chemical reagents, photo-catalysts and electrochemical or solvothermal methods have been used. Chua *et al.*[9] discussed a range of reducing agents and compared the C/O ratios and the conductivity attainable as a measure of the effectiveness of the different procedures employed.

For the large-scale reduction of GO, the most widely used procedures include chemical and thermal reduction. Other less commonly used approaches include enzymatic, electrochemical reduction, light catalyzed reduction and plasma-assisted methods as discussed in previous reviews.[9]

Chemical reduction

Such processes are attractive and a wide range of reducing agents has been studied for the chemical reduction of GO in view of the processes being inherently scalable.[9] One of the most common chemical reductants is hydrazine, for which the ability to control pH during the reduction enables a surfactant-free scalable preparation of aqueous dispersions (Table 3).[10,50,62]

Pham *et al.*[63] studied the effect of temperature on the extent of GO reduction by hydrazine. The reduction of GO at low temperatures (< 30–50 °C) resulted in highly dispersible CCG in organic solvents. CCG obtained from GO reduction at 30 °C is dispersible in *N*-methyl-2-pyrrolidone concentrations in as high as 0.71 mg ml^{-1}. A free-standing paper made of this CCG possessed an electrical conductivity of more than 220 S cm^{-1}.
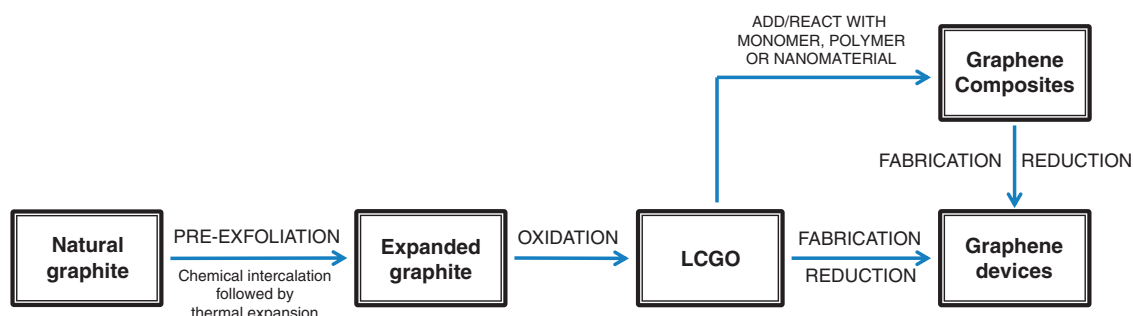
Anhydrous stable dispersions of CCG in dimethylformamide can be prepared by redispersing hydrazine-reduced GO in the dimethyl formamide with triethylamine.[64] The same approach can be used to disperse a more highly reduced CCG that has been prepared by reducing GO by using both hydrazine and ammonia at 220 °C under pressure for 2 h.[64] This highly reduced CCG was shown to have an O_{1S}/C_{1S} ratio of 0.06, which approaches that of graphite. These CCGs with varying degrees of reduction form dispersions in anhydrous dimethyl formamide that are stable for several months at concentrations of 0.5–0.6 mg ml^{-1}.

Less toxic alternatives to hydrazine include ascorbic acid and sulphur compounds ($NaHSO_3$, $SOCl_2$, SO_2) (Table 3). For example,

Table 3 Selected examples of various GO reducing conditions along with the properties of the resulting CCG

Reducing agent	Dispersion medium	Conc. (mg ml^{-1})	C/O ratio	Sheet size (µm)/ height profile (nm)	Conductivity (S cm^{-1})	Conditions of reduction	Ref.
Hydrazine	H$_2$O	0.5	10.3	~0.4–0.5/1	72	95 °C	57
Hydrazine	Binary (DMF/H$_2$O—9:1 v/v)	0.3	11.0	~0.5/0.7–0.8	17	1 µl per 3 mg of GO for 12 h at 80 °C	59
Hydrazine	NMP	0.71	9.58	—	220	24 h at 30–50 °C	63
	DMF	0.64					
	PC	0.66					
Hydrazine	Anhydrous DMF	0.6	16.6	~0.4/0.9	99.4	4 h at 230 °C	64
L-ascorbic acid	H$_2$O, DMF and NMP	0.1	12.5	~0.5/1.0	99.6	2 mM for 15 min	115
HI/AcOH	DMF	0.3	6.7	—	304	40 h at 40 °C	66
NH$_3$-borane	THF and H$_2$O	0.02–0.2	9.8–14.2	—	203	3–12 h at 80 °C	67
NaHSO$_3$	H$_2$O/DMAc = 1:6	—	6.68	>1/0.79–0.87	65	95 °C for 3 h	65

Abbreviations: CCG, chemically converted graphene; DMAc, N,N-dimethylacetamide; DMF, dimethylformamide; NMP, N-methyl-2-pyrrolidone; PC, propylene carbonate; THF, tetrahydrofuran.

Figure 3 Steps involved in forming graphene composites or devices via liquid crystalline graphene oxide formation.

a 0.05 mg ml^{-1} dispersion of GO was reduced in a binary mixture of dimethylacetamide (DMAc)/H$_2$O using NaHSO$_3$. When redispersed in DMAc/H$_2$O, the resulting graphene powder gave a stable dispersion that was used to fabricate foils with a conductivity of 65 S cm^{-1}.[65] The highest conductivities of CCG have been reported after chemical reduction of GO using a HI/AcOH reductant and are as high as 304 S cm^{-1} with high C/O ratios of up to 15.[10,66] This can be achieved with both solutions and films of GO. An NH$_3$-borane reduction method has also been used resulting in aqueous or organic dispersions with a reported conductivity of 203 S cm^{-1} for fabricated foils.[67] Some of these processes are limited due to the low concentration of dispersion that can be processed.

Thermal reduction
Since heat may have a role in processing and fabrication procedures, the effect of this is the degree of reduction of GO Should be considered. It has been shown that rapid heating of GO ($\geqslant$2000 ° C min^{-1}) resulted in exfoliated sheets wherein decomposition of oxygen bearing functionalities was noted. This dual effect makes thermal expansion of graphite oxide a promising route for bulk processing. Schniepp et al.[40] observed that below 500 °C, the C/O ratio for the product obtained was no more than 7, and with temperatures that reached 750 °C, the C/O ratio was higher than 13. Li et al.[68] observed an effect of thermal annealing of foils prepared from aqueous dispersions of CCG. Conductivity improved from ~40 to ~350 S cm^{-1} after treatment at 500 °C.

Microwave treatment provides a promising approach for the efficient large-scale production of CCG sheets. The main advantage of microwave irradiation over other conventional heating methods is that the heating of the reaction mixture is uniform and rapid.

A rapid rise in temperature due to the difference in the solvent/ substrates and reactant dielectric constants can provide significant enhancement in the transfer of energy directly to the reactants. The microwave-assisted synthesis of Fe-decorated rGO by in situ reduction of ferrocene has been reported.[69] A rGO/poly(amidoamine)-silver nanoparticle composite was synthesized by in situ reduction of both AgNO$_3$ and GO under microwave irradiation.[70] The development of a stacked electrode supercapacitor cell using single-walled nanotubes/ microwave exfoliated GO composites as electrode material has been reported.[71] A composite material consisting of GO exfoliated under microwave radiation and manganosite (MnO) was synthesized to explore their potential as electrode material.[72]

LIQUID CRYSTALLINE DISPERSIONS OF GRAPHENE OXIDE
Natural graphite is the source of choice for LCGO production. The common approaches to exfoliate GO, discussed earlier, apply extensive mechanical forces such as sonication that break down the GO sheets usually to sub-micron sizes. However, GO should have a lateral sheet size greater than a few microns to be able to form a LC dispersion at practical concentrations.[2] The synthesis of large GO sheets is dependent on two factors: the use of a starting material with large graphite flakes and the avoidance of strong mechanical forces such as vigorous ultrasonication.[56] Pre-exfoliated graphite or expanded graphite has been the most common precursor for making large GO sheets as the open pores of the expanded graphite facilitates the exfoliation process and makes exfoliation possible even by simple stirring.[3,56] The steps involved in fabricating graphene containing
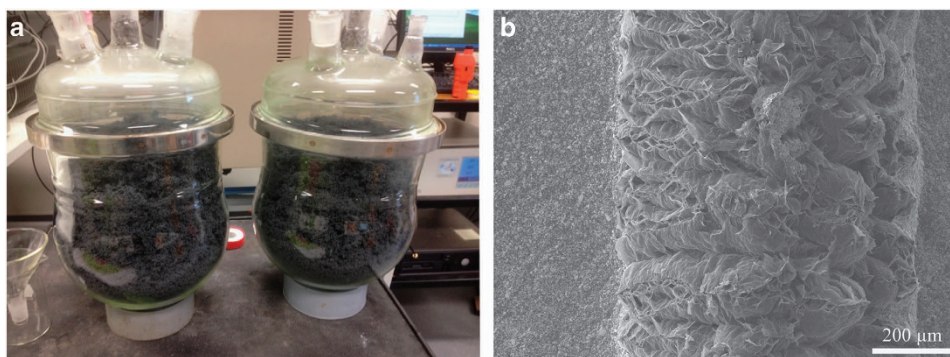
Figure 4 (**a**) Intercalated graphite after rapid thermal expansion at 700 °C, prepared in the Australian Research Council Centre of Excellence for Electromaterials Science (University of Wollongong) laboratories. (**b**) Scanning electron microscope image of thermally expanded graphite.

structures via the formation and utilization of LCGO dispersions are summarized in Figure 3.

Thermal expansion of intercalated graphite
Open pores and very thin graphite layers in thermally expanded graphite has made chemical solution exfoliation possible through stirring. Therefore, expanded graphite was found to be the best precursor for making GO containing large sheets.[52,60] The most common choice of intercalation compound is graphite bisulphate, which can be expanded along the c-axis *via* rapid thermal heating at 1050 °C for 15 s.[3,16,56] This rapid heating, results in thermal decomposition of the intercalants into gaseous species that overcomes the van der Waals attractions and forces the carbon layers apart. During thermal expansion, the graphite expands up to ~ 300 times along the *c* axis to transform the graphite platelets into worm shaped expanded graphite (Figure 4).

The scanning electron microscope image of thermally expanded graphite (Figure 4b) shows that although the graphene layers are exfoliated, they still have partial connection to adjacent layers. It should be noted that a minimum graphite particle size of 75 μm is required for an efficient intercalation and expansion. If the particles are not large enough, they mostly are oxidized on the edge rather than intercalation occurring, and the expansion is negligible.[73] Therefore, natural graphite with a large grain size (that is, Asbury Carbons 3772) is the source of choice for thermal expansion and LCGO production.

The production of LCGO is practically very important for the fabrication of graphene-containing devices as the LC state can be utilized to direct the inherent ordered assembly of GO in macroscopic structures via industrially scalable methods such as spinning, printing and coating.[4,21,52] Jalili *et al.*[2] have addressed the key features of GO sheets governing the formation of LCGO dispersions and their processability. They have suggested that the competition between orientational and positional entropy in large sheets is the driver for LC formation in GO dispersions. In their study, the LC phase was found to form in dispersions containing large sheets, whereas the dispersion of small GO sheets supports isotropic phase formation as illustrated in Figure 5.

Figure 6 presents images of large GO sheets that were prepared using expanded graphite. The dispersion contained ultra-large GO sheets with an average lateral size of 37 μm that formed LC dispersions at concentrations less than 1 mg ml^{-1}, which is far less than any other colloidal dispersion.[3,56] It is possible to evaluate the formation of LCGO using polarized optical microscopy. Under crossed-polarizers, the LCGO shows birefringence typical of lyotropic liquid crystals, as shown in Figure 6d.

Formation of LCGO in various organic solvents is very exciting as liquid crystals in organic solvents offer new possibilities to develop potentially useful materials such as conductive inks, and to achieve chemical reactions with non-water soluble reactants. Jalili *et al.*,[52] have reported the formation of LCGO in a large range of organic solvents including ethanol, acetone, tetrahydrofuran, *N*-dimethylformamide, *N*-cyclohexyl-2-pyrrolidone and a number of other organic solvents. Before the introduction of LCGO in organic solvents, the number of solvents that could support the LC phase was restricted to a very limited range of multifunctional alcohols (such as ethylene glycol), amides and a wide range of protic ionic liquids. In the case of LCGO, its extraordinarily high aspect ratio and ability to form multiple hydrogen bonds enables the formation of the LC phase in a wide range of organic solvents, which were previously thought to be unable to support LC phases. Figure 7 shows representative polarized optical microscopy micrographs of LCGO in some selected organic solvents.

GRAPHENE POLYMER COMPOSITES
A detailed review on composite materials based on CCG has been produced by Bai *et al.*[74] Advances in graphene/polymer composites using other types of graphene have also been reviewed.[75–78]

Two general approaches can be taken to the introduction of CCG into polymers as previously described;[74] a GO polymer composite can be initially formed with subsequent reduction of the GO or the pre-formed CCG can be introduced into the polymer. Within in each of these general approaches there can be considerable variation in how the polymer is introduced, whether by mixing or *in situ* polymerization that may lead to covalently bound nanocomposites. In all cases, restacking of the nanocarbon sheets must be minimized in order to produce composites with improved, mechanical and electrical properties.[76] These approaches are briefly discussed below.

Solution mixing
In attempting to form a polymer composite with dispersed graphenes, a common solvent for the polymer and the GO or CCG dispersion is required. Introduction of the polymer should not cause graphene aggregation. Table 4 summarizes examples of the outcomes from solution mixing various graphenes and polymers using organic or aqueous solvents. GO or CCG is dispersed in a suitable solvent like water, acetone, chloroform, tetrahydrofuran, dimethyl formamide or toluene, the polymer adsorbed on to the GO or CCG sheets, *in situ* reduction undertaken as necessary and the solvent evaporated.

The formation of a variety of poly(vinyl alcohol) (PVA)-nanocarbon composites by this method (Table 4) highlights the value of this simple solution approach. GO sheets can be easily dispersed in
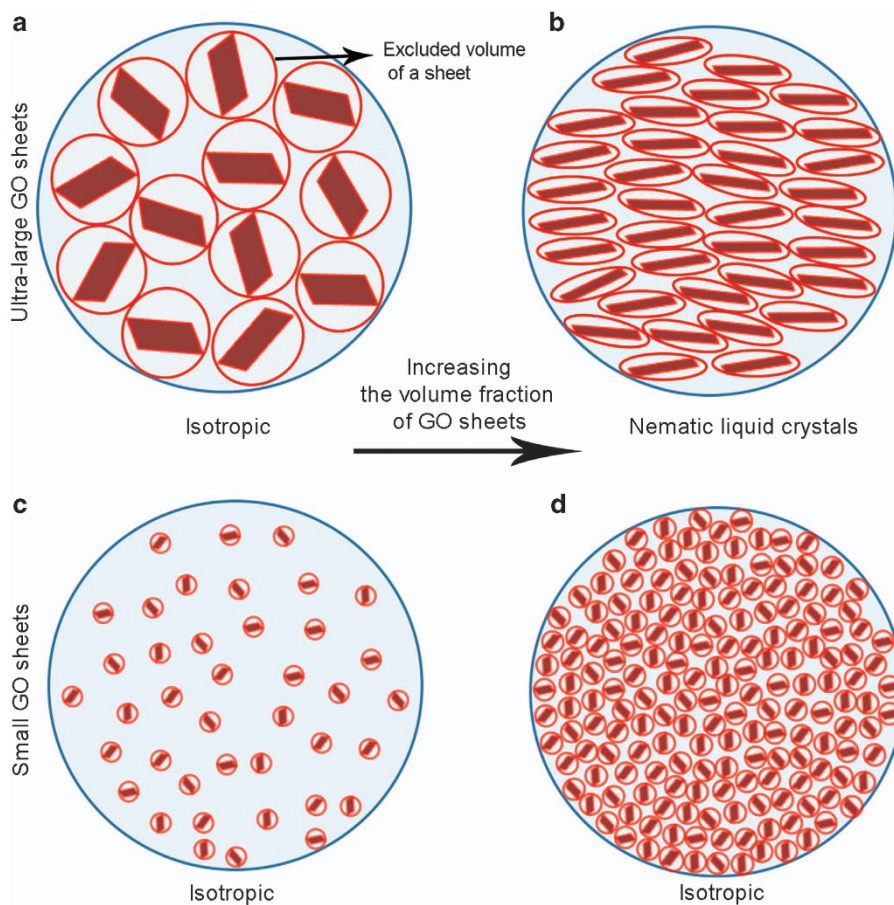
Figure 5 Evolution of liquid crystalline phases in graphene oxide dispersions containing large sheet size upon increasing the concentration. (**a**) At low concentrations, large graphene oxide sheets are randomly dispersed in the solution exhibiting large excluded volume. (**b**) Upon increasing the concentration, the sheets orientate parallel to each other in order to minimize the excluded volume and consequently form nematic order. (**c**) At the low concentration regime, small graphene oxide sheets form a fully isotropic phase. (**d**) An increase in concentration does not induce spontaneous packing of the nematic phase.[2] Reproduced by permission from The Royal Society of Chemistry.

aqueous media and the mechanical properties and thermal stability of composites with hydrophilic polymers such as poly(ethylene oxide) (PEO) and PVA can be improved. Thus, using a simple and environmental friendly water solution processing method, Yang *et al.*[79] prepared PVA-GO composite films. The tensile strength of the 2 wt% PVA-GO composite film increased sharply by 92.2% from 22 to 42 MPa and the modulus by 167% from 0.45 to 1.21 GPa. These significant improvements are attributed to the homogeneous dispersion of GO in the polymer matrix, strong H-bonding and effective load transfer across the PVA-GO interface. These improvements are similar to those obtained by Zhao *et al.*[80] for a PVA-graphene composite, prepared by reducing the GO *in situ*.

In contrast, the tensile strength of PVA-GO fibers, prepared by a simple coagulation spinning technique, was found to be 240 MPa by Wang *et al.*[81] and could be improved even further (80%) by the addition of single walled nanotubes (SWNTs). As for the PVA-nanocarbon composite film work described above, reduction of the GO to graphene did not significantly affect the tensile strength although the fiber elasticity was dramatically improved. Notwithstanding this, the use of pre-formed graphene (an aqueous dispersion of CCG) to form a composite with SWNTs and PVA gives dramatically improved toughness in wet spun fibers (see later).[27]

Similar improvements in hydrogel properties can be achieved by the simple solution mixing of aqueous CCG with a biomaterial such as chitosan. Sayyar *et al.*[82] have demonstrated that CCG/chitosan composites containing up to 3% graphene show large improvements in conductivity and mechanical properties but retain the processability and swellability of the polymer matrix. This results in a robust, conducting biocompatible material that can be extrusion-printed into 3D scaffolds.

As is evident from the other selected examples in Table 4, large improvements in the properties of a wide variety of polymers can be achieved by the simple solution mixing of GO or graphene with the polymer.[26,83–87]

Melt intercalation

Melt extrusion/mechanical blending is one of the most economical and commercially viable methods for graphene nanocomposite preparation. During this process, the graphene fillers are dispersed in a thermoplastic polymer matrix without solvent using a shear force at elevated temperatures by conventional methods such as extrusion and injection moulding.[76] Many researchers report using a melt mixing process with the polymer and GO that is thermally reduced to graphene during the mixing process rather than a pre-prepared CCG. However, thermally reduced GO can produce graphene that is reduced in size and significantly distorted, leading to a lower conductivities and poorer mechanical property improvements. In this regard, Kim *et al.* compared melt compounding, solvent mixing and *in situ* polymerization of GO
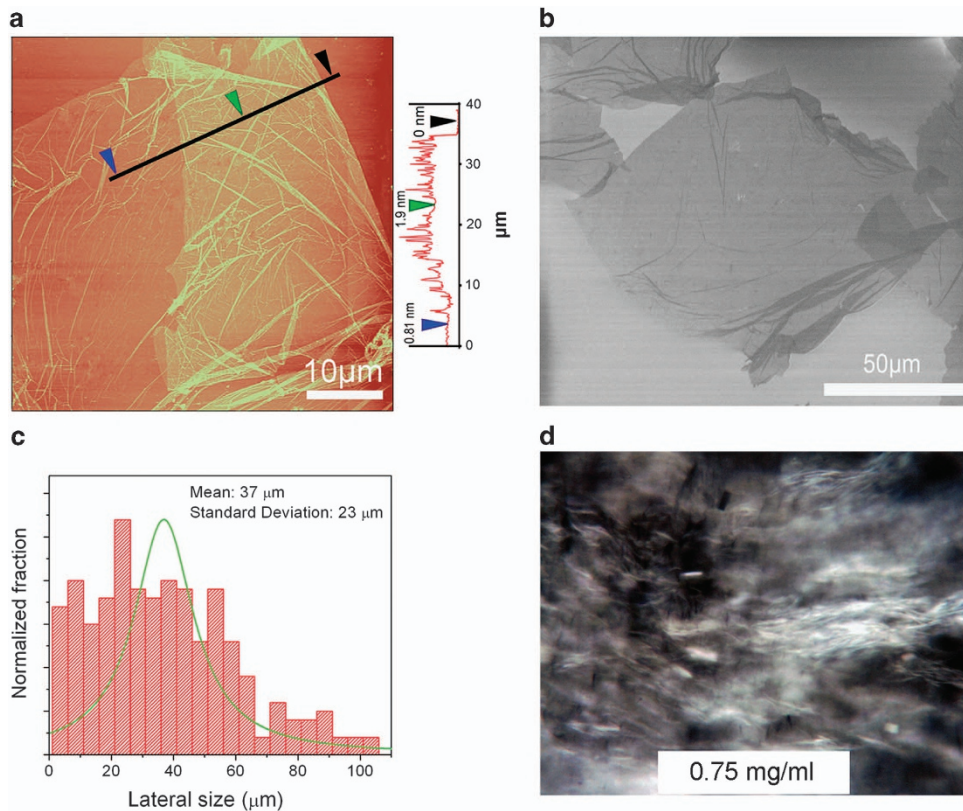
Figure 6 (**a**) Atomic force microscopy image of a large graphene oxide sheet. (**b**) Representative scanning electron microscopy images of graphene oxide sheets. (**c**) The corresponding lateral size distribution of graphene oxide sheets. (**d**) Representative polarized optical microscopy image of liquid crystalline graphene oxide at a graphene oxide concentration as low as 0.75 mg ml^{-1}. Reprinted with permission from Aboutalebi et al.[56]. Copyright 2011 WILEY-VCH Verlag GmbH & Co KGaA, Weinheim.

Figure 7 Representative polarized optical microscopy micrographs of liquid crystalline graphene oxide in various organic solvents at a graphene oxide concentration of 2.5 mg ml^{-1}. Reprinted with permission from Aboutalebi et al.[52] Copyright 2013 American Chemical Society.

and functionalized GO with thermoplastic polyurethane.[88] They found that solution processing was more effective in distributing the thermally reduced graphene through the polymer matrix than melt processing. This resulted in a decrease in the amount of graphene required in the solution-processed composite (<0.3 vol%) to achieve the same conductivity as the melt processed composite (>0.5 vol%). This difference in composite properties was considered to be outweighed by the ease and lower cost of the polymer extrusion process.

More recently, Wang et al.[89] prepared multilayer graphene-filled poly(vinyl chloride) composites using conventional melt-mixing

Table 4 Selected examples of solution mixing of graphenes with polymers to form polymer composites

Polymer form of graphene[a]	Graphene dispersion solvent	Nanocarbon amount	Processing	Properties of the composite	Ref.
PVA-GO	H_2O	0.5–2%	Solution	Tensile stress and modulus of 2% composite increase by 92 and 167%, respectively.	79
PVA-rGO	H_2O containing 0.5 wt % SDBS	0.3–3%	In situ reduction	Tensile strength of 1.8 vol% graphene composite increases by 150%.	80
PVA-GO/SWNT and PVA-rGO/SWNT (fibers)	H_2O (<pH 2)	3.5 mg/ml	Solution and in situ reduction	Tensile strength increase of 80 and 133% increase in the elastic modulus over pure GO fibers are obtained with a 2:1 (v/v) ratio of SWCNT to GO.	81
PVA-CCG/SWNT (fibers)	DMF	0.3 wt.% CCG and 0.3 wt.% SWNT	Solution	Fibers with gravimetric toughness that approaches $1000 \, J \, g^{-1}$.	27
Polyimide-GO	DMAc	0.3–5.0%	Solution and thermal	Tensile strength (844 MPa), Young's modulus (50.5 GPa).	83
PS-GO and PS-rGO	H_2O	0.1–2%	Solution and in situ reduction	PS microspheres wrapped with graphene nanosheets with low percolation threshold and good conductivity.	84
PVC-GO	THF	0.5–3.0%	Solution and sonication	Quality factor improvement from 22 to 100%.	85
Chitosan-CCG	H_2O	0.1–3.0%	Solution and sonication	3% Graphene hydrogel tensile strength increase of 60% in swollen state and 7× higher elongation at break. Material can be extrusion printed.	82
Polyurethane-GNS[b]	DMF	0.1–2.0%	In situ reduction	Improvement in tensile strength and storage modulus by 239 and 202%.	86
Polycaprolactone-CCG	DMF	0.1–5.0%	Solution and chemical	Compares covalently attached and mixed. Improved homogeneity, mechanical and conducting (13 orders of magnitude increase) properties.	26
Natural rubber-rGO	H_2O	2.5–10.0%	Solution sonication and in situ reduction	~50% improvement in tensile strength.	87

Abbreviations: CCG, chemically converted graphene; DMAc, N,N-dimethylacetamide; DMF, dimethylformamide; GO, graphene oxide; GNS, graphene nanosheets; PI, polyimide; PS, polystyrene; PU, polyurethane; PVA, poly(vinyl alcohol); PVC, poly(vinyl chloride); rGO, reduced graphene oxide; SDBS, sodium dodecylbenzenesulfonate; SWNT, single-walled nanotube; THF, tetrahydrofuran.
[a]Graphene oxides and reduced graphene oxides.
[b]GNS obtained from the reduction of GO.

methods that demonstrated a much lower friction co-efficient and wear rate than pristine poly(vinyl chloride) as a result of the enhanced toughness of the nanocomposites and the self-lubricating nature of the graphene.

Some variations on this approach have been reported to improve the flexural properties, electrical conductivity and percolation threshold of the resulting polymer nanocomposite. For example, Kalaitzidou et al.[90] have demonstrated that initial coating of the polymer particles by the nanocarbon using sonication in a solvent provides an improved melt intercalated product, in this case polypropylene reinforced with exfoliated graphite nanoplatelets. Zhan et al.[87] compared the rGO-rubber composite prepared by solution mixing and melt intercalation. There was a marginal improvement in the mechanical properties by melt intercalation as compared with solvent mixing.

In situ polymerization
Using this approach, CCG is produced or mixed with the monomer, a suitable initiator is added if necessary and polymerization induced by either by heat or radiation.[74] This approach has been limited by the lack of availability of stable CCG dispersions in organic solvents in the presence of monomer. Therefore, in situ polymerization has most commonly been effected in the presence of GO with simultaneous thermal reduction to graphene. For example, polymerization of caprolactam in the presence of GO resulting in graphene-reinforced Nylon-6 composite[91] in which the nylon chains are grafted onto both the basal plane and periphery of the graphene. As a result, the tensile strength of fibers prepared by melt spinning of the Nylon-graphene composite were increased 2.1-fold and the Young's modulus 2.4-fold with a graphene loading of only 0.1%.[91]

The availability of stable dispersions of CCG particularly in organic solvents has led to the covalent attachment of polymers to CCG by way of in situ polymerization. Sayyar et al. have prepared covalently functionalized polycaprolactone-CCG composites and compared them with the analogous solution processed composites. The covalently linked composites exhibit far better homogeneity and as a result, both Young's modulus and tensile strength more than double with significant improvement in conductivity.[92] In vitro cytotoxicity testing of the materials showed good biocompatibility resulting in promising materials for use as conducting substrates for the electrically stimulated growth of cells.

Chemical functionalization
Chemical functionalization of either GO or CCG can be utilized to improve the solubility/dispersibility of the nanocarbon as well as its interactions with the polymer. This can involve simply attaching groups to the nanocarbon to improve its noncovalent interactions with the polymer, covalently attaching the polymer to the graphene or providing reactive functionality on the graphene from which to form the polymer. Considerable work has been carried out in this area and the reader is directed to a number of significant reviews on this topic.[93–97]

FABRICATION OF GRAPHENE-CONTAINING STRUCTURES AND DEVICES
Accompanying the development of processable graphenes has been substantial interest in the fabrication of graphene-based functional devices using printing (ink-jet and extrusion) and fiber spinning. The key challenges in printing and spinning graphene are production of suitable graphene dispersions, formulation of these dispersions into

printing inks or spinning solutions and a fabrication technique. In the following section, an overview of the recent progress regarding printing and spinning of graphene and its composites is given.

Inkjet printing

Inkjet printing has been widely employed as an efficient technique for the patterning of graphene sheets for the fabrication a variety of flexible electronic devices such as a wideband dipole-antenna,[98] gas sensor[99] and acoustic actuator electrodes.[100] The inks used in these applications comprise aqueous GO either thermally or chemically reduced following printing and can be directly patterned on various flexible substrates such as poly(ethylene terephthalate) film and paper in high resolution. Moreover, the transparency and conductivity of the patterns can be simply controlled by the concentration of the GO-based ink or the number of print passes.[101] In order to formulate a printable graphene-based ink, high solubility, suitable viscosity and low dispersion surface tension are critical parameters.[102,103]

To inkjet print a CCG dispersion, it is usually mixed with surfactant to modify the surface tension and solubility,[99] in contrast to GO-based inks that have no solubility issues and can be mixed with organic solvents to adjust their surface tension.[4,98] For example, a PVA-CCG composite has been used for inkjet printing of organic field-effect transistors. Using the PVA as a stabilizer made it possible to formulate a stable and printable CCG-based ink at low concentrations.[104]

Extrusion printing of 3D structures

Extrusion printing provides a versatile alternative for the fabrication of graphene patterns and 3D structures by depositing a graphene solution or molten composite, containing a thermoplastic polymer, onto a selected substrate using a mechanically driven or pneumatically pressurized extruder.[105] In this system, standard computer aided design software is used to design patterns and geometries followed by extrusion printing of the customized architectures. In the case of graphene dispersions, the rheology of the ink needs to be controlled by concentration,[4] whereas, for the composite, the polymer aids the processing.[92] CCG has been used in printed patterns for the fabrication of flexible electronics,[106] and in a composite with poly-caprolactone as a melt extruded scaffold for tissue engineering.[92] In this latter paper, graphene/PCl composite fibers (Figures 8a and b) were extrusion printed onto a glass substrate to form circular 3D scaffolds (Figure 8c). Figure 8d shows a similarly sized scaffold with alternating matched concentric circles of graphene/PCl composite fibers and pristine PCl fibers that can be used to examine the effects of cell growth in regions under electrical stimulation for tissue engineering.

Wet-spinning

Wet-spinning is a fabrication process that can be used to create fibers from a vast range of organic materials including conducting polymers,[107] carbon nanotubes[108] and graphene.[3] The production of graphene fibers using wet-spinning has added a new dimension to graphene processing and fabrication. In this method, a solution containing graphene is injected through a spinneret in a bath containing a non-solvent, which results in solidification of the graphene fiber as it emerges into the coagulation bath. Graphene fibers exploit the inherent properties of a graphene sheet and have the type of macroscopic structure required for practical applications such as high performance supercapacitors and batteries.

In order to wet-spin CCG, composite production is typically required. With this approach, CCG is added to modify the electrical, electrochemical and mechanical properties of the final fibers. Kim and co-workers,[27] have reported production of tough composite fibers from CCG/CNTs/PVA. The gravimetric toughness approaches $1000 \, J \, g^{-1}$, far exceeding spider dragline silk ($165 \, J \, g^{-1}$) and Kevlar
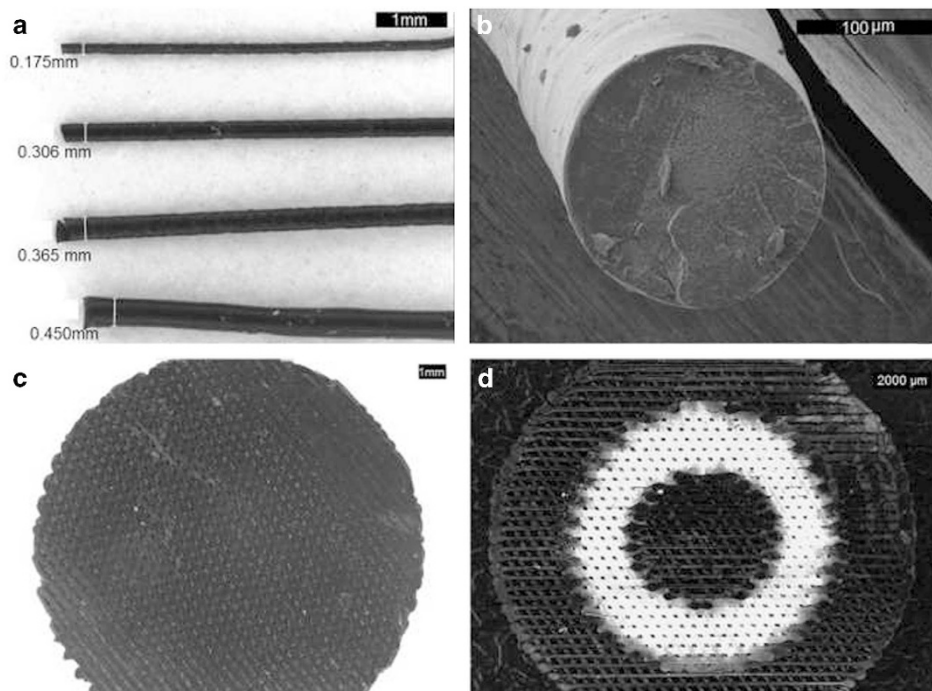

Figure 8 (**a**) Printed graphene/PCl fibers with different diameters. (**b**) Cross-section of extruded PCl fibers. (**c**) Graphene/PCl composite printed in the form of a scaffold consisting fibers with a thickness of $220 \, \mu m$ and a pore-size of $130 \, \mu m$. (**d**) Graphene/PCl composite and pristine PCl printed in the form of a combined scaffold. Reprinted with permission from Sayyar *et al*.[92]
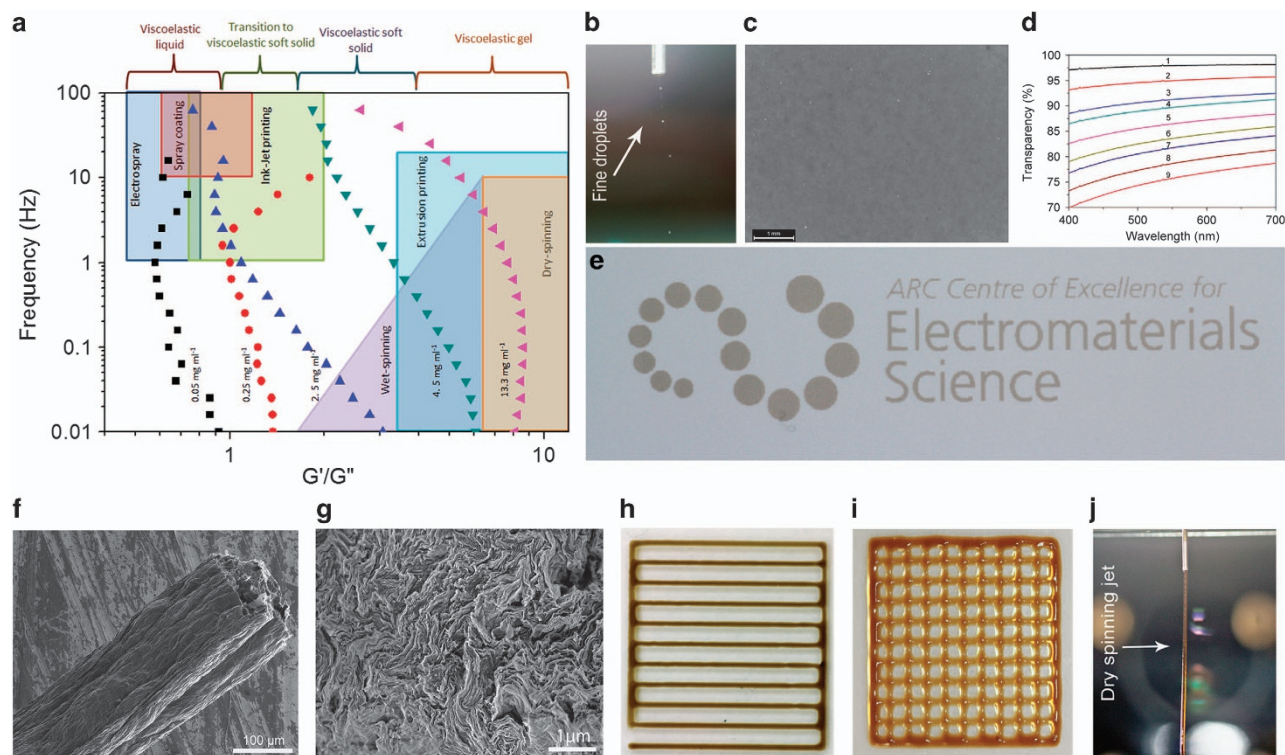
Figure 9 (**a**) A correlation between rheological properties and the key prerequisites for various manufacturing techniques enabled fabrication of liquid crystalline graphene oxide via a wide range of industrial techniques. Overlaid are the approximate processing regimes for a number of industrial fabrication techniques. (**b**) Photograph of electrospraying of a viscoelastic liquid of graphene oxide dispersion at a concentration of 0.05 mg ml^{-1}. (**c**) Photograph of a graphene oxide thin film that was spray coated and thermally reduced utilizing a transitional state to viscoelastic liquid graphene oxide dispersion of 0.25 mg ml^{-1}. (**d**) Transparency of the spray coated-reduced graphene oxide thin films as a function of coating layers; the numbers show the number of coating layers. (**e**) Ink-jet printed logo using liquid crystalline graphene oxide viscoelastic soft solid at a concentration of 0.75 mg ml^{-1}. (**f**) As-prepared wet-spun fibers from liquid crystalline graphene oxide viscoelastic soft solid at a concentration of 2.5 mg ml^{-1}. (**g**) Cross-section of a wet-spun liquid crystalline graphene oxide fiber, showing that graphene oxide sheets are stacked in layers with some degree of folding and are ordered due to the formation of nematic liquid crystals. (**h**) Extrusion printed pattern using liquid crystalline graphene oxide viscoelastic gel of 4.5 mg ml^{-1}. (**i**) Extrusion printed three-dimensional architecture using liquid crystalline graphene oxide viscoelastic gel of 13.3 mg ml^{-1}. (**j**) Dry-spinning of liquid crystalline graphene oxide fibers utilizing liquid crystalline graphene oxide viscoelastic gel of 13.3 mg ml^{-1}.[4] Reproduced by permission of The Royal Society of Chemistry.

(78 J g^{-1}). This toughness enhancement is consistent with the observed formation of an interconnected network of partially aligned CCG flakes and CNTs during solution spinning. The CCG/polymer composite fibers are twice as strong and able to absorb 15 times higher energy before rupture than previously reported graphene/polymer composites. After removal of the polymer, the graphene fibers presented a high electrochemical capacitance.

In contrast, composite-free CCG fibers can be obtained by wet spinning LCGO dispersions and thermally or chemically reducing the resulting fibers. As demonstrated by three recent studies, the larger the GO sheets, the better the fiber mechanical properties.[3,109,110] These studies highlight the unique features of LCGO that make it remarkably useful for the fabrication of a variety of graphene structures.

LCGO—a versatile material for fabrication

LCGO has added a new dimension to soft self-assembly science and graphene fabrication. The recent understanding of the flow behavior and tuning the rheology of the LCGO dispersion have expanded the range of possible industrial scalable fabrication techniques for graphene to spinning (wet and dry), printing (ink-jet and extrusion) and coatings (spray and electrospray).[4] In this context, a series of graphene-based macroscopic structures such as strong and highly conducting fibers and high performance supercapacitors have been fabricated employing LCGO.[3,21]

The key advantage of LCGO is its self-alignment. The controllable rheology of LCGO dispersions make them ideal for fiber fabrication. During a process such as wet-spinning, the orientation induced by the LC phase, combined with the additional contribution of the flow field, creates highly ordered domains that result in strong structures without the need for drawing and post-fabrication treatments.[3]

The LC state can be exploited to direct the ordered assembly of graphene sheets in macroscopic structures via scalable fabrication methods without the need of additional polymer or binder to aid the processing.[4] Therefore, LCGO can be fabricated by itself to produce neat and high performance graphene architectures. It has been shown that, over the change in the concentration, LCGO undergoes four distinct rheological regions from a viscoelastic liquid, a transition state consisting of viscoelastic liquid and viscoelastic soft solid, viscoelastic soft solid and viscoelastic gel.[4] Each of these unbinding regions is suitable for unique industrial processing techniques (Figure 9). When the viscous modulus (G'') dominates, the GO dispersion is suitable for high rate processing methods where the dispersion must spread on contact with the substrate such as spray coating and inkjet printing (Figures 9a–e). On the other hand, when the elastic modulus (G') is high, the rheological properties suit fabrication methods requiring the dispersion to keep its given shape, such as extrusion printing and fiber spinning (Figures 9e–j).[4]

CONCLUSIONS/FUTURE TRENDS

Standing on the shoulders of the carbon nanotube experience, graphene has been catapulted onto a stage where the drive and desire for commercial returns is intense. That drive and desire is for now tempered by a lack of knowledge in key areas that can take us from graphite source to graphene-containing products in an environmentally sustainable manner.

Matching and tweaking the myriad of chemistries available to the source of graphite is the first critical step. Critical processes not addressed in this review are the steps involved between mining graphite to its purification and intercalation, which usually involves mechanical separation and flotation, chemical (acid/alkali) and/or high temperature treatment to get up >99.9% carbon, a prerequisite for processable graphene dispersions production; with a view to bulk processing, there is a need for exfoliation of graphite that uses environmentally friendly processes and minimizes oxidation, without sacrificing quality.

Developing improved non-toxic GO reduction procedures resulting in high dispersion concentration in both aqueous and organic media, matching chemistries that enhance functional properties and do not compromise processing, graphene scaleup and device fabrication are all areas that continue to require a significant research focus.

Extensive effort world-wide is in the direction of commercializing graphene technology. This is a result of massive government funding[1] along with a growing number of commercial manufacturers producing a wide range of graphene products.

The potential of graphene is in no doubt and many of the chemistries discussed here will undoubtedly be translated into processes that lead to graphene-containing products. What will be exciting will be to see how diverse the use of CCGs will become once these chemistries have been established.

CONFLICT OF INTEREST

The authors declare no conflict of interest.

ACKNOWLEDGEMENTS

1   Peplow, M. Graphene: the quest for supercarbon. *Nature* **503**, 327–329 (2013).
2   Jalili, R., Aboutalebi, S. H., Esrafilzadeh, D., Konstantinov, K., Razal, J. M., Moulton, S. E. & Wallace, G. G. Formation and processability of liquid crystalline dispersions of graphene oxide. *Mater. Horiz* **1**, 87–91 (2014).
3   Jalili, R., Aboutalebi, S. H., Esrafilzadeh, D., Shepherd, R. L., Chen, J., Aminorroaya-Yamini, S., Konstantinov, K., Minett, A. I., Razal, J. M. & Wallace, G. G. Scalable one-step wet-spinning of graphene fibers and yarns from liquid crystalline dispersions of graphene oxide: towards multifunctional textiles. *Adv. Funct. Mater.* **10**, 5345–5354 (2013).
4   Naficy, S., Jalili, R., Aboutalebi, S. H., Gorkin, R., Konstantinov, K., Innis, P. C., Spinks, G. M., Poulin, P. & Wallace, G. G. Graphene oxide dispersions: tuning rheology to enable fabrication. *Mater. Horiz* **1**, 326–331 (2014).
5   Novoselov, K. S., Geim, A. K., Morozov, S. V., Jiang, D., Zhang, Y., Dubonos, S. V., Grigorieva, I. V. & Firsov, A. A. Electric field effect in atomically thin carbon films. *Science* **306**, 666–669 (2004).
6   Park, S. & Ruoff, R. S. Chemical methods for the production of graphenes. *Nat. Nanotechnol.* **4**, 217–224 (2009).
7   Allen, M. J., Tung, V. C. & Kaner, R. B. Honeycomb carbon: a review of graphene. *Chem. Rev.* **110**, 132–145 (2009).
8   Wassei, J. K. & Kaner, R. B. Oh, the places you'll go with graphene. *Acc. Chem. Res.* **46**, 2244–2253 (2013).
9   Chua, C. K. & Pumera, M. Chemical reduction of graphene oxide: a synthetic chemistry viewpoint. *Chem. Soc. Rev.* **43**, 291–312 (2014).
10 Pei, S. & Cheng, H.-M. The reduction of graphene oxide. *Carbon* **50**, 3210–3228 (2012).
11 Sherrell, P. C., Thompson, B. C., Wassei, J. K., Gelmi, A. A., Higgins, M. J., Kaner, R. B. & Wallace, G. G. Maintaining cytocompatibility of biopolymers through a graphene layer for electrical stimulation of nerve cells. *Adv. Funct. Mater.* **24**, 769–776 (2014).
12 Bae, S., Kim, H., Lee, Y., Xu, X., Park, J.-S., Zheng, Y., Balakrishnan, J., Lei, T., Ri Kim, H., Song, Y. I., Kim, Y.-J., Kim, K. S., Ozyilmaz, B., Ahn, J.-H., Hong, B. H. & Iijima, S. Roll-to-roll production of 30-inch graphene films for transparent electrodes. *Nat. Nanotechnol.* **5**, 574–578 (2010).
13 Eda, G., Fanchini, G. & Chhowalla, M. Large-area ultrathin films of reduced graphene oxide as a transparent and flexible electronic material. *Nat. Nanotechnol.* **3**, 270–274 (2008).
14 Kim, K. S., Zhao, Y., Jang, H., Lee, S. Y., Kim, J. M., Kim, K. S., Ahn, J.-H., Kim, P., Choi, J.-Y. & Hong, B. H. Large-scale pattern growth of graphene films for stretchable transparent electrodes. *Nature* **457**, 706–710 (2009).
15 Wang, C., Li, D., Too, C. O. & Wallace, G. G. Electrochemical properties of graphene paper electrodes used in lithium batteries. *Chem. Mater.* **21**, 2604–2606 (2009).
16 Aboutalebi, S. H., Chidembo, A. T., Salari, M., Konstantinov, K., Wexler, D., Liu, H. K. & Dou, S. X. Comparison of GO, GO/MWCNTs composite and MWCNTs as potential electrode materials for supercapacitors. *Energy Environ. Sci.* **4**, 1855–1865 (2011).
17 Zhu, Y., Murali, S., Stoller, M. D., Ganesh, K. J., Cai, W., Ferreira, P. J., Pirkle, A., Wallace, R. M., Cychosz, K. A., Thommes, M., Su, D., Stach, E. A. & Ruoff, R. S. Carbon-based supercapacitors produced by activation of graphene. *Science* **332**, 1537–1541 (2011).
18 El-Kady, M. F., Strong, V., Dubin, S. & Kaner, R. B. Laser scribing of high-performance and flexible graphene-based electrochemical capacitors. *Science* **335**, 1326–1330 (2012).
19 Yang, Y., Wang, C., Yue, B., Gambhir, S., Too, C. O. & Wallace, G. G. Electrochemically synthesized polypyrrole/graphene composite film for lithium batteries. *Adv. Energy Mater.* **2**, 266–272 (2012).
20 Yang, X., Cheng, C., Wang, Y., Qiu, L. & Li, D. Liquid-mediated dense integration of graphene materials for compact capacitive energy storage. *Science* **341**, 534–537 (2013).
21 Aboutalebi, S. H., Jalili, R., Esrafilzadeh, D., Salari, M., Gholamvand, Z., Aminorroaya Yamini, S., Konstantinov, K., Shepherd, R. L., Chen, J., Moulton, S. E., Innis, P. C., Minett, A. I., Razal, J. M. & Wallace, G. G. High-performance multifunctional graphene yarns: toward wearable all-carbon energy storage textiles. *ACS Nano* **8**, 2456–2466 (2014).
22 Li, S., Zhao, C., Shu, K., Wang, C., Guo, Z., Wallace, G. G. & Liu, H. Mechanically strong high performance layered polypyrrole nano fibre/graphene film for flexible solid state supercapacitor. *Carbon* **79**, 554–562 (2014).
23 Shu, K., Wang, C., Wang, M., Zhao, C. & Wallace, G. G. Graphene cryogel papers with enhanced mechanical strength for high performance lithium battery anodes. *J. Mater. Chem. A* **2**, 1325–1331 (2014).
24 Haag, D. R. & Kung, H. H. Metal-free graphene based catalysts: a review. *Top. Catal.* **57**, 762–773 (2014).
25 Yavari, F. & Koratkar, N. Graphene-based chemical sensors. *J. Phys. Chem. Lett.* **3**, 1746–1753 (2012).
26 Sayyar, S., Murray, E., Thompson, B. C., Gambhir, S., Officer, D. L. & Wallace, G. G. Covalently linked biocompatible graphene/polycaprolactone composites for tissue engineering. *Carbon* **52**, 296–304 (2013).
27 Shin, M. K., Lee, B., Kim, S. H., Lee, J. A., Spinks, G. M., Gambhir, S., Wallace, G. G., Kozlov, M. E., Baughman, R. H. & Kim, S. J. Synergistic toughening of composite fibres by self-alignment of reduced graphene oxide and carbon nanotubes. *Nat. Commun.* **3**, 650 (2012).
28 Kim, J., Cote, L. J. & Huang, J. Two dimensional soft material: new faces of graphene oxide. *Acc. Chem. Res.* **45**, 1356–1364 (2012).
29 Wissler, M. Graphite and carbon powders for electrochemical applications. *J. Power Sources* **156**, 142–150 (2006).
30 Celzard, A., Marêché, J. F. & Furdin, G. Modelling of exfoliated graphite. *Prog. Mater. Sci.* **50**, 93–179 (2005).
31 Cai, M., Thorpe, D., Adamson, D. H. & Schniepp, H. C. Methods of graphite exfoliation. *J. Mater. Chem.* **22**, 24992–25002 (2012).
32 Dresselhaus, M. S. & Dresselhaus, G. Intercalation compounds of graphite. *Adv. Phys.* **51**, 1–186 (2002).
33 Dresselhaus, M. S. & Dresselhaus, G. Intercalation compounds of graphite. *Adv. Phys.* **30**, 139–326 (1981).
34 Viculis, L. M., Mack, J. J., Mayer, O. M., Hahn, H. T. & Kaner, R. B. Intercalation and exfoliation routes to graphite nanoplatelets. *J. Mater. Chem.* **15**, 974–978 (2005).
35 Chen, G., Wu, D., Weng, W. & Wu, C. Exfoliation of graphite flake and its nanocomposites. *Carbon* **41**, 619–621 (2003).
36 Inagaki, M. On the formation and decomposition of graphite-bisulfate. *Carbon* **4**, 137–141 (1966).
37 Edwards, R. S. & Coleman, K. S. Graphene synthesis: relationship to applications. *Nanoscale* **5**, 38–51 (2013).
38 Fu, W., Kiggans, J., Overbury, S. H., Schwartz, V. & Liang, C. Low-temperature exfoliation of multilayer-graphene material from FeCl3 and CH3NO2 co-intercalated graphite compound. *Chem. Commun.* **47**, 5265–5267 (2011).
39 McAllister, M. J., Li, J.-L., Adamson, D. H., Schniepp, H. C., Abdala, A. A., Liu, J., Herrera-Alonso, M., Milius, D. L., Car, R., Prud'homme, R. K. & Aksay, I. A. Single sheet functionalized graphene by oxidation and thermal expansion of graphite. *Chem. Mater.* **19**, 4396–4404 (2007).

40 Schniepp, H. C., Li, J.-L., McAllister, M. J., Sai, H., Herrera-Alonso, M., Adamson, D. H., Prud'homme, R. K., Car, R., Saville, D. A. & Aksay, I. A. Functionalized single graphene sheets derived from splitting graphite oxide. *J. Phys. Chem. B* **110**, 8535–8539 (2006).

41 Mao, M., Chen, S., He, P., Zhang, H. & Liu, H. Facile and economical mass production of graphene dispersions and flakes. *J. Mater. Chem. A* **2**, 4132–4135 (2014).

42 Staudenmaier, L. Verfahren zur Darstellung der Graphitsäure. *Ber. Dtsch. Chem. Ges* **32**, 1394–1399 (1899).

43 Hummers, W. S. Jr. & Offeman, R. E. Preparation of graphitic oxide. *J. Am. Chem. Soc.* **80**, 1339 (1958).

44 Kovtyukhova, N. I., Ollivier, P. J., Martin, B. R., Mallouk, T. E., Chizhik, S. A., Buzaneva, E. V. & Gorchinskiy, A. D. Layer-by-layer assembly of ultrathin composite films from micron-sized graphite oxide sheets and polycations. *Chem. Mater.* **11**, 771–778 (1999).

45 Dreyer, D. R., Park, S., Bielawski, C. W. & Ruoff, R. S. The chemistry of graphene oxide. *Chem. Soc. Rev.* **39**, 228–240 (2010).

46 Zhu, Y., Murali, S., Cai, W., Li, X., Suk, J. W., Potts, J. R. & Ruoff, R. S. Graphene and graphene oxide: synthesis, properties, and applications. *Adv. Mater.* **22**, 3906–3924 (2010).

47 Wang, Y., Shi, Z., Yu, J., Chen, L., Zhu, J. & Hu, Z. Tailoring the characteristics of graphite oxide nanosheets for the production of high-performance poly(vinyl alcohol) composites. *Carbon* **50**, 5525–5536 (2012).

48 Shao, G., Lu, Y., Wu, F., Yang, C., Zeng, F. & Wu, Q. Graphene oxide: the mechanisms of oxidation and exfoliation. *J. Mater. Sci.* **47**, 4400–4409 (2012).

49 Marcano, D. C., Kosynkin, D. V., Berlin, J. M., Sinitskii, A., Sun, Z., Slesarev, A., Alemany, L. B., Lu, W. & Tour, J. M. Improved synthesis of graphene oxide. *ACS Nano* **4**, 4806–4814 (2010).

50 Li, D., Mueller, M. B., Gilje, S., Kaner, R. B. & Wallace, G. G. Processable aqueous dispersions of graphene nanosheets. *Nat. Nanotechnol.* **3**, 101–105 (2008).

51 Cai, D. & Song, M. Preparation of fully exfoliated graphite oxide nano platelets in organic solvents. *J. Mater. Chem.* **17**, 3678–3680 (2007).

52 Jalili, R., Aboutalebi, S. H., Esrafilzadeh, D., Konstantinov, K., Moulton, S. E., Razal, J. M. & Wallace, G. G. Organic solvent-based graphene oxide liquid crystals: a facile route toward the next generation of self-assembled layer-by-layer multifunctional 3D architectures. *ACS Nano* **7**, 3981–3990 (2013).

53 Mueller, M. B., Quirino, J. P., Nesterenko, P. N., Haddad, P. R., Gambhir, S., Li, D. & Wallace, G. G. Capillary zone electrophoresis of graphene oxide and chemically converted graphene. *J. Chromatogr. A* **1217**, 7593–7597 (2010).

54 Ogino, I., Yokoyama, Y., Iwamura, S. & Mukai, S. R. Exfoliation of graphite oxide in water without sonication: bridging length scales from nanosheets to macroscopic materials. *Chem. Mater.* **26**, 3334–3339 (2014).

55 Zhang, C., Lv, W., Xie, X., Tang, D., Liu, C. & Yang, Q.-H. Towards low temperature thermal exfoliation of graphite oxide for graphene production. *Carbon* **62**, 11–24 (2013).

56 Aboutalebi, S. H., Gudarzi, M. M., Zheng, Q. B. & Kim, J.-K. Spontaneous formation of liquid crystals in ultralarge graphene oxide dispersions. *Adv. Funct. Mater.* **21**, 2978–2988 (2011).

57 Balandin, A. A., Ghosh, S., Bao, W., Calizo, I., Teweldebrhan, D., Miao, F. & Lau, C. N. Superior thermal conductivity of single-layer graphene. *Nano Lett.* **8**, 902–907 (2008).

58 Gudarzi, M. M., Moghadam, M. H. M. & Sharif, F. Spontaneous exfoliation of graphite oxide in polar aprotic solvents as the route to produce graphene oxide—organic solvents liquid crystals. *Carbon* **64**, 403–415 (2013).

59 Park, S., An, J., Jung, I., Piner, R. D., An, S. J., Li, X., Velamakanni, A. & Ruoff, R. S. Colloidal suspensions of highly reduced graphene oxide in a wide variety of organic solvents. *Nano Lett.* **9**, 1593–1597 (2009).

60 Pham, V.-H., Cuong, T.-V., Nguyen-Phan, T.-D., Pham, H.-D., Kim, E.-J., Hur, S.-H., Shin, E.-W., Kim, S.-W. & Chung, J.-S. One-step synthesis of superior dispersion of chemically converted graphene in organic solvents. *Chem. Commun.* **46**, 4375–4377 (2010).

61 Stankovich, S., Piner, R. D., Nguyen, S. T. & Ruoff, R. S. Synthesis and exfoliation of isocyanate-treated graphene oxide nanoplatelets. *Carbon* **44**, 3342–3347 (2006).

62 Tung, V. C., Allen, M. J., Yang, Y. & Kaner, R. B. High-throughput solution processing of large-scale graphene. *Nat. Nanotechnol* **4**, 25–29 (2009).

63 Pham, V. H., Dang, T. T., Cuong, T. V., Hur, S. H., Kong, B.-S., Kim, E. J. & Chung, J. S. Synthesis of highly concentrated suspension of chemically converted graphene in organic solvents: effect of temperature on the extent of reduction and dispersibility. *Korean J. Chem. Eng.* **29**, 680–685 (2012).

64 Gambhir, S., Murray, E., Sayyar, S., Wallace, G. G. & Officer, D. L. Anhydrous organic dispersions of highly reduced chemically converted graphene. *Carbon* **76**, 368–377 (2014).

65 Chen, W.-F., Yan, L.-F. & Bangal, P. R. Chemical reduction of graphene oxide to graphene by sulfur-containing compounds. *J. Phys. Chem. C* **114**, 19885–19890 (2010).

66 Moon, I. K., Lee, J., Ruoff, R. S. & Lee, H. Reduced graphene oxide by chemical graphitization. *Nat. Commun.* **1**, 73 (2010).

67 Pham, V. H., Hur, S. H., Kim, E. J., Kim, B. S. & Chung, J. S. Highly efficient reduction of graphene oxide using ammonia borane. *Chem. Commun.* **49**, 6665–6667 (2013).

68 Chen, H., Müller, M. B., Gilmore, K. J., Wallace, G. G. & Li, D. Mechanically strong, electrically conductive, and biocompatible graphene paper. *Adv. Mater.* **20**, 3557–3561 (2008).

69 Gollavelli, G. & Ling, Y.-C. Multi-functional graphene as an *in vitro* and *in vivo* imaging probe. *Biomaterials* **33**, 2532–2545 (2012).

70 Luo, Z., Yuwen, L., Han, Y., Tian, J., Zhu, X., Weng, L. & Wang, L. Reduced graphene oxide/PAMAM-silver nanoparticles nanocomposite modified electrode for direct electrochemistry of glucose oxidase and glucose sensing. *Biosens. Bioelectron.* **36**, 179–185 (2012).

71 Antiohos, D., Pingmuang, K., Romano, M. S., Beirne, S., Romeo, T., Aitchison, P., Minett, A., Wallace, G., Phanichphant, S. & Chen, J. Manganosite-microwave exfoliated graphene oxide composites for asymmetric supercapacitor device applications. *Electrochim. Acta* **101**, 99–108 (2013).

72 Antiohos, D., Romano, M. S., Razal, J. M., Beirne, S., Aitchison, P., Minett, A. I., Wallace, G. G. & Chen, J. Performance enhancement of single-walled nanotube-microwave exfoliated graphene oxide composite electrodes using a stacked electrode configuration. *J. Mater. Chem. A* **2**, 14835–14843 (2014).

73 Chung, D. D. L. Exfoliation of graphite. *J. Mater. Sci.* **22**, 4190–4198 (1987).

74 Bai, H., Li, C. & Shi, G. Functional composite materials based on chemically converted graphene. *Adv. Mater.* **23**, 1089–1115 (2011).

75 Das, T. K. & Prusty, S. Graphene-based polymer composites and their applications. *Polym. Plast. Technol. Eng* **52**, 319–331 (2013).

76 Du, J. & Cheng, H.-M. The fabrication, properties, and uses of graphene/polymer composites. *Macromol. Chem. Phys.* **213**, 1060–1077 (2012).

77 Huang, X., Qi, X., Boey, F. & Zhang, H. Graphene-based composites. *Chem. Soc. Rev.* **41**, 666–686 (2012).

78 Kim, H., Abdala, A. & Macosko, C. W. Graphene/polymer nanocomposites. *Macromolecules* **43**, 6515–6530 (2010).

79 Yang, X., Shang, S. & Li, L. Layer-structured poly(vinyl alcohol)/graphene oxide nanocomposites with improved thermal and mechanical properties. *J. Appl. Polym. Sci.* **120**, 1355–1360 (2011).

80 Zhao, X., Zhang, Q., Chen, D. & Lu, P. Enhanced mechanical properties of graphene-based poly(vinyl alcohol) composites. *Macromolecules* **43**, 2357–2363 (2010).

81 Wang, R.-R., Sun, J., Gao, L., Xu, C.-H. & Zhang, J. Fibrous nanocomposites of carbon nanotubes and graphene-oxide with synergetic mechanical and actuative performance. *Chem. Commun.* **47**, 8650–8652 (2011).

82 Sayyar, S., Murray, E., Thompson, B. C., Chung, J., Officer, D. L., Gambhir, S., Spinks, G. M. & Wallace, G. G. Processable conducting graphene/chitosan hydrogels for tissue engineering. *J. Mater. Chem. B* **3**, 481–490 (2015).

83 Wang, J.-Y., Yang, S.-Y., Huang, Y.-L., Tien, H.-W., Chin, W.-K. & Ma, C.-C. M. Preparation and properties of graphene oxide/polyimide composite films with low dielectric constant and ultrahigh strength via *in situ* polymerization. *J. Mater. Chem.* **21**, 13569–13575 (2011).

84 Yang, L., Wang, Z., Ji, Y., Wang, J. & Xue, G. Highly ordered 3d graphene-based polymer composite materials fabricated by 'particle-constructing' method and their outstanding conductivity. *Macromolecules* **47**, 1749–1756 (2014).

85 Joshi, G. M. & Deshmukh, K. Optimized quality factor of graphene oxide-reinforced PVC nanocomposite. *J. Electron. Mater.* **43**, 1161–1165 (2014).

86 Wang, X., Hu, Y., Song, L., Yang, H., Xing, W. & Lu, H. *In situ* polymerization of graphene nanosheets and polyurethane with enhanced mechanical and thermal properties. *J. Mater. Chem.* **21**, 4222–4227 (2011).

87 Zhan, Y., Wu, J., Xia, H., Yan, N., Fei, G. & Yuan, G. Dispersion and exfoliation of graphene in rubber by an ultrasonically-assisted latex mixing and *in situ* reduction process. *Macromol. Mater. Eng.* **296**, 590–602 (2011).

88 Kim, H., Miura, Y. & Macosko, C. W. Graphene/polyurethane nanocomposites for improved gas barrier and electrical conductivity. *Chem. Mater.* **22**, 3441–3450 (2010).

89 Wang, H., Xie, G., Zhu, Z., Ying, Z. & Zeng, Y. Enhanced tribological performance of the multi-layer graphene filled poly (vinyl chloride) composites. *Composites Part A* **67**, 268–273 (2014).

90 Kalaitzidou, K., Fukushima, H. & Drzal, L. T. A new compounding method for exfoliated graphite-polypropylene nanocomposites with enhanced flexural properties and lower percolation threshold. *Compos. Sci. Technol* **67**, 2045–2051 (2007).

91 Xu, Z. & Gao, C. *In situ* polymerization approach to graphene-reinforced nylon-6 composites. *Macromolecules* **43**, 6716–6723 (2010).

92 Sayyar, S., Cornock, R., Murray, E., Beirne, S., Officer, D. L. & Wallace, G. G. Extrusion printed graphene/polycaprolactone/composites for tissue engineering. *Mater. Sci. Forum* **773-774**, 496–502 (2014).

93 Kuilla, T., Bhadra, S., Yao, D., Kim, N. H., Bose, S. & Lee, J. H. Recent advances in graphene based polymer composites. *Prog. Polym. Sci.* **35**, 1350–1375 (2010).

94 Potts, J. R., Murali, S., Zhu, Y., Zhao, X. & Ruoff, R. S. Microwave-exfoliated graphite oxide/polycarbonate composites. *Macromolecules* **44**, 6488–6495 (2011).

95 Salavagione, H. J., Martinez, G. & Ellis, G. Recent advances in the covalent modification of graphene with polymers. *Macromol. Rapid Commun.* **32**, 1771–1789 (2011).

96 Potts, J. R., Dreyer, D. R., Bielawski, C. W. & Ruoff, R. S. Graphene-based polymer nanocomposites. *Polymer* **52**, 5–25 (2011).

97 Liu, J., Tanga, J. & Gooding, J. J. Strategies for chemical modification of graphene and applications of chemically modified graphene. *J. Mater. Chem.* **22**, 12435–12452 (2012).

98 Shin, K.-Y., Hong, J.-Y. & Jang, J. Micropatterning of graphene sheets by inkjet printing and its wideband dipole-antenna application. *Adv. Mater.* **23**, 2113–2118 (2011).

99 Dua, V., Surwade, S. P., Ammu, S., Agnihotra, S. R., Jain, S., Roberts, K. E., Park, S., Ruoff, R. S. & Manohar, S. K. All-organic vapor sensor using inkjet-printed reduced graphene oxide. *Angew. Chem., Int. Ed. Engl.* **49**, 2154–2157 (2010).

100 Shin, K.-Y., Hong, J.-Y. & Jang, J. Flexible and transparent graphene films as acoustic actuator electrodes using inkjet printing. *Chem. Commun.* **47**, 8527–8529 (2011).

101 Hong, J.-Y. & Jang, J. Micropatterning of graphene sheets: recent advances in techniques and applications. *J. Mater. Chem.* **22**, 8179–8191 (2012).

102 Calvert, P. Inkjet printing for materials and devices. *Chem. Mater.* **13**, 3299–3305 (2001).

103 Derby, B. Inkjet printing of functional and structural materials: fluid property requirements, feature stability, and resolution. *Annu. Rev. Mater. Res.* **40**, 395–414 (2010).

104 Lim, S., Kang, B., Kwak, D., Lee, W. H., Lim, J. A. & Cho, K. Inkjet-printed reduced graphene oxide/poly(vinyl alcohol) composite electrodes for flexible transparent organic field-effect transistors. *J. Phys. Chem. C* **116**, 7520–7525 (2012).

105 Cornock, R., Beirne, S. & Wallace, G. G. *2013 IEEE/ASME International Conference on Advanced Intelligent Mechatronics (AIM)* 973–978 (IEEE, Wollongong, Australia, 2013).

106 Tölle, F. J., Fabritius, M. & Mülhaupt, R. Emulsifier-free graphene dispersions with high graphene content for printed electronics and freestanding graphene films. *Adv. Funct. Mater.* **22**, 1136–1144 (2012).

107 Jalili, R., Razal, J. M., Innis, P. C. & Wallace, G. G. One-step wet-spinning process of poly(3, 4-ethylenedioxythiophene): poly(styrenesulfonate) fibers and the origin of higher electrical conductivity. *Adv. Funct. Mater.* **21**, 3363–3370 (2011).

108 Lu, W., Zu, M., Byun, J. H., Kim, B. S. & Chou, T. W. State of the art of carbon nanotube fibers: opportunities and challenges. *Adv. Mater.* **24**, 1805–1833 (2012).

109 Xu, Z. & Gao, C. Graphene chiral liquid crystals and macroscopic assembled fibres. *Nat. Commun.* **2**, 571 (2011).

110 Xu, Z., Sun, H., Zhao, X. & Gao, C. Ultrastrong fibers assembled from giant graphene oxide sheets. *Adv. Mater.* **25**, 188–193 (2013).

111 Stankovich, S., Dikin, D. A., Piner, R. D., Kohlhaas, K. A., Kleinhammes, A., Jia, Y., Wu, Y., Nguyen, S. T. & Ruoff, R. S. Synthesis of graphene-based nanosheets via chemical reduction of exfoliated graphite oxide. *Carbon* **45**, 1558–1565 (2007).

112 Dimiev, A. M., Alemany, L. B. & Tour, J. M. Graphene oxide: origin of acidity, instability in water, and new dynamic structural model. *ACS Nano* **7**, 576–588 (2013).

113 Liu, F., Sun, J., Zhu, L., Meng, X., Qi, C. & Xiao, F.-S. Sulfated graphene as an efficient solid catalyst for acid-catalyzed liquid reactions. *J. Mater. Chem.* **22**, 5495–5502 (2012).

114 Dimiev, A. M. & Tour, J. M. Mechanism of graphene oxide formation. *ACS Nano* **8**, 3060–3068 (2014).

115 Fernandez-Merino, M. J., Guardia, L., Paredes, J. I., Villar-Rodil, S., Solis-Fernandez, P., Martinez-Alonso, A. & Tascon, J. M. D. Vitamin C is an ideal substitute for hydrazine in the reduction of graphene oxide suspensions. *J. Phys. Chem. C* **114**, 6426–6432 (2010).

Dr Sanjeev Gambhir obtained his PhD from the Council of Scientific and Industrial Research laboratory, India in 1988. He started his career with industry and worked with Ranbaxy Research Laboratory in its R&D division. He left the industry as Head of Custom Synthesis Division in 2000 and he joined the Nanomaterials Research Centre, Massey University, Palmerston North, New Zealand as a post-doctoral fellow. His research interests focused on developing new functionalized polythiophene-based conducting polymers and porphyrin dyes. In 2007, he joined Dyesol, Australia and successfully set up the pilot scale facility for the syntheses of kilograms quantities of dyes and intermediates. Since 2008, he has worked in the Intelligent Polymer Research Institute and the Materials Node of the Australian National Fabrication Facility at the University of Wollongong. His research has been focused on the chemical oxidation of graphite and developing graphene/polymer composites for a variety of applications. He has over 31 publications in peer reviewed journals.

Dr Rouhollah Jalili is an engineer and a material chemist holding a graphene development fellowship from the Australian Research Council Centre of Excellence for Electromaterials Science. He obtained his BSc and MSc in Engineering from the Isfahan University of Technology, Iran. Thereafter, he received his PhD degree from the Intelligent Polymer Research Institute at the University of Wollongong in 2013. His research breakthrough was the demonstration of the key role of graphene oxide liquid crystals in the fabrication of multifunctional graphene-based architecture using industrially scalable techniques such as wet-spinning, electrospinning, printing (ink-jet and extrusion) and coatings. He has also developed solvophobic soft self-assembly of graphene oxide sheets in a wide range of organic solvents, which provides a platform for tailor-making self-assembled and self-oriented graphene-based composites with large-area molecular ordering. His current research focus includes the development and fabrication of graphene and other two-dimensional materials for application in flexible electronic and bionic devices.

Professor David Officer is Professor of Organic Chemistry in the Intelligent Polymer Research Institute and the Australian Research Council Centre of Excellence for Electromaterials Science at the University of Wollongong, Wollongong, Australia. He obtained his PhD in Chemistry at Victoria University of Wellington, Wellington, New Zealand in 1982, working with Professor Brian Halton. He joined the lecturing staff at Massey University, New Zealand in 1986 after 3 years of research work in organic chemistry with Professor Ron Warrener at The Australian National University in Canberra, Australia and as an Alexander von Humboldt Fellow with Professor Emanuel Vogel at the University of Cologne in Germany. During his 22 years at Massey University, he became the founding Director of the Nanomaterials Research Centre and Professor in Chemistry in the Institute of Fundamental Sciences. In 2007, he moved to the University of Wollongong. He has published more than a 150 papers in the areas of graphene, porphyrin and conducting polymer chemistry, nanomaterials and solar cells.

Professor Gordon Wallace is currently the Executive Research Director at the Australian Research Council (ARC) Centre of Excellence for Electromaterials Science and Director of the Intelligent Polymer Research Institute. He previously held an ARC Federation Fellowship and currently holds an ARC Laureate Fellowship. Professor Wallace's research interests include organic conductors, nanomaterials and electrochemical probe methods of analysis and the use of these in the development of Intelligent Polymer Systems, with a particular focus on the development and application of additive fabrication of these materials. A current focus involves the use of these tools and materials in developing bio-communications from the molecular to skeletal domains in order to improve human performance via medical bionics. He has published more than 700 refereed publications, including monographs on *Conductive Electroactive Polymers: Intelligent Polymer Systems* (3rd Edition 2009) and *Organic Bionics* (2012) and an ebook on *3D Bioprinting*.